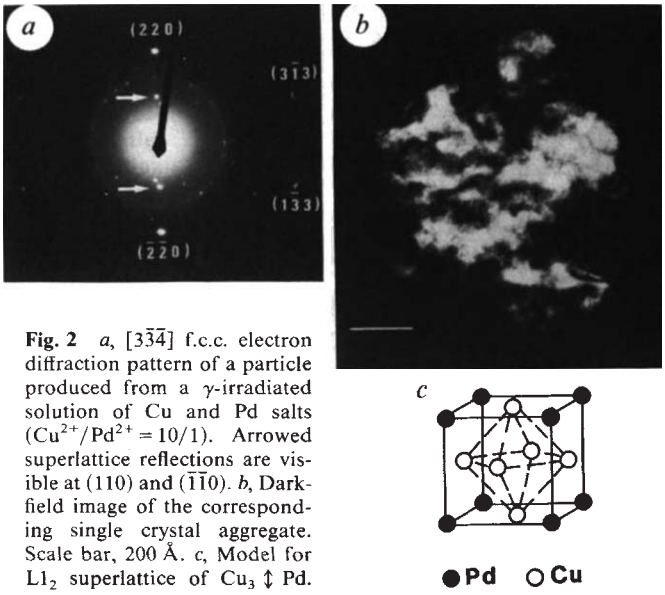

Fig. 2 *a*, [3$\bar{3}\bar{4}$] f.c.c. electron diffraction pattern of a particle produced from a γ-irradiated solution of Cu and Pd salts ($Cu^{2+}/Pd^{2+} = 10/1$). Arrowed superlattice reflections are visible at (110) and ($\bar{1}\bar{1}$0). *b*, Dark-field image of the corresponding single crystal aggregate. Scale bar, 200 Å. *c*, Model for $L1_2$ superlattice of Cu_3 ↕ Pd.

Pure nickel: A solution of $NiSO_4$ 2×10^{-3} mol l^{-1} in de-aerated water containing isopropanol 0.2 mol l^{-1} and PVA 0.2 mol l^{-1} (base monomer) has been irradiated at natural $pH = 6.8$ up to 205 kGy (20.5 Mrad). Chemical analysis was carried out under nitrogen in a glove-box, by reduction of nitro-blue tetrazolium chloride into monoformazan kept in solution due to PVA and measured by optical absorption. The radiolytic yield, 0.03 Ni atoms per 100 eV, is much lower than for Pt (ref. 6). (Other conditions can be found which lead to much higher values of Ni yield, but so far at most 50% Ni^{2+} has been reduced to metallic Ni (J.B., J.P.C., M.O.D. and J.L.M., in preparation). The subcolloidal solution is brown and highly reactive towards air, but the dried particles can be kept in air without further oxidation as shown by electron diffraction. Figure 1 is a TEM micrograph showing the distribution of polycrystalline clumps of size ranging from ~100 to 200 Å. The clumps appear to be embedded in an amorphous substance which may be polymer, but which remains to be identified. Electron diffraction shows Debye rings which can be indexed as Ni. f.c.c. structure (face-centred cubic). Small-angle rings are also observed but it has proved impossible to classify these as oxide, hydroxide or sulphate. Higher-magnification dark-field images show that the clumps are made up of several crystal grains of 50–100 Å in size, which appear to have twin relation[18].

Cu–Pd alloy: A de-aerated solution containing $CuSO_4$ 10^{-3} mol l^{-1}, $PdCl_2$ 10^{-4} mol l^{-1}, isopropanol 0.56 mol l^{-1} and PVA 0.1 mol l^{-1}, pH 10.2 has been irradiated up to 8 kGy. The colloid has a dark green colour (while a pure Cu sol is pink). TEM observations show a very inhomogeneous distribution of particle sizes (ranging from a few hundred Å to ~1 μm) and structures. Figure 2*a* is an electron diffraction pattern from a large single crystal aggregate, imaged in Fig. 2*b*, which can be indexed as the [3$\bar{3}\bar{4}$] orientation of the f.c.c. reciprocal lattice. Moreover, clear superlattice reflections (arrowed) are visible at (110) and ($\bar{1}\bar{1}$0). This corresponds to the $L1_2$ superlattice (Fig. 2*c*) of stoichiometric Cu_3Pd. We have also obtained diffraction patterns suggesting a b.c.c. structure (body-centred cubic) and superlattice as well as unknown f.c.c. superlattice; in all cases these clearly imply ordered atomic arrangements. Note that when the initial Cu^{2+}/Pd^{2+} ratio is 1 instead of 10 the CuPd superlattice has been observed.

In proper conditions, radiation-induced reduction can produce a wide variety of highly divided metallic materials either pure or alloyed. Extensive applications of these materials are likely to be found, as well as new alloy phases and structures.

We thank J. Amblard for valuable discussions and Mrs M. Miñana for technical assistance. This work was supported under the auspices of CNRS, contract ATP 2045.

Received 4 March; accepted 17 July 1985.

1. Haissinsky, M. in *Radiation Chemistry* (eds Dobo, J. & Hedvig, P.) 1353–1365 (Akademiai Kiado, Budapest, 1972).
2. Delcourt, M. O. & Belloni, J. *Radiochem. radioanalyt. Lett.* **13**, 329–338 (1973).
3. Henglein, A. *Ber. Bunsenges. phys. Chem.* **81**, 556–561 (1977).
4. Henglein, A. & Tausch-Treml, R. *J. Colloid Interface* **80**, 84–93 (1981).
5. Fujita, H., Isawa, M. & Yamazaki, H. *Nature* **196**, 666–667 (1962).
6. Belloni, J., Delcourt, M.O. & Leclere, C. *Nouv. J. Chim.* **6**, 507–509 (1982).
7. Delcourt, M. O., Belloni, J., Marignier, J. L., Mory, C. & Colliex, C. *Radiat. Phys. Chem.* **23**, 485–487 (1983).
8. Delcourt, M. O., Keghouche, N. & Belloni, J. *Nouv. J. Chim.* **7**, 131–136 (1983).
9. Belloni-Cofler, J., Marigner, J. L., Delcourt-Euverte, M. O. & Miñana-Lourseau, M. CNRS French Patent, 84.09196 (13 June 1984).
10. Henglein, A. *J. phys. Chem.* **83**, 2858–2862 (1979).
11. Butler, J. & Henglein, A. *Radiat. phys. Chem.* **15**, 603–612 (1980).
12. Buxton, G. V., Rhodes, T. & Sellers, R. M. *JCS Faraday Trans. I.* **78**, 3341–3356 (1982).
13. Henglein. A. *Ber. Bunsenges. phys. Chem.* **84**, 253–259 (1980).
14. Anbar, M., Bambeneck, M. & Ross, A. B. *Nat. Stand. Ref. Data Ser., Nat. Bur. Stand.* **43** (1973).
15. Ross, A. B. *Nat. Stand. Ref. Data Ser., Nat. Bur. Stand.* **43**, Suppl. (1975).
16. Kelm, M., Lilie, J., Henglein, A. & Janata, E. *J. phys. Chem.* **78**, 882–887 (1974).
17. Freiberg, M. & Meyerstein, D. *JCS Faraday Trans. I* **73**, 622–631 (1977).
18. Marks, L. D. & Smith, D. J. *J. Microsc.* **130**, 249–261 (1983).

Franciscan Complex Calera limestones: accreted remnants of Farallon Plate oceanic plateaus

John A. Tarduno*, Michael McWilliams*, Michel G. Debiche*, William V. Sliter† & M. C. Blake Jr†

* Department of Geophysics, Stanford University, Stanford, California 94305, USA
† US Geological Survey, Menlo Park, California 94025, USA

The Calera Limestone, part of the Franciscan Complex of northern California, may have formed in a palaeoenvironment similar to Hess and Shatsky Rises of the present north-west Pacific[1]. We report here new palaeomagnetic results, palaeontological data and recent plate-motion models that reinforce this assertion. The Calera Limestone may have formed on Farallon Plate plateaus, north of the Pacific–Farallon spreading centre as a counterpart to Hess or Shatsky Rises. In one model[2], the plateaus were formed by hotspots close to the Farallon–Pacific ridge axis. On accretion to North America, plateau dissection in the late Cretaceous to Eocene (50–70 Myr) could explain the occurrence of large volumes of pillow basalt and exotic blocks of limestone in the Franciscan Complex. Partial subduction of the plateaus could have contributed to Laramide (70–40 Myr) compressional events[3].

The Aptian to Coniacian (115–88 Myr) Calera Limestone occurs in coastal California as a belt of blocks in the Permanente Terrane[4] (Fig. 1). In addition to the limestone, the terrane contains pillow basalt, radiolarian chert of lower Cretaceous (Valanginian) age and continentally-derived greywackes and shale. The limestone is dominantly pelagic, but rare shallow-water oolitic and bioclastic rocks are also found[5]. Pelagic limestone is interbedded locally with pillow lava, tuffaceous breccia, and volcanic sandstone.

The Calera Limestone has two facies, one a light grey limestone interbedded with replacement chert, the other a bituminous black facies. The black facies is lithologically similar to mid-Cretaceous anoxic zones seen on Manihiki Plateau, Hess Rise and Shatsky Rise. This observation led Jenkyns[1] to infer a common depositional environment for the Franciscan and oceanic rocks, and to assign a provisional Cenomanian age to the anoxic part of the Calera Limestone. Together with Pacific plate reconstructions, results from the Deep Sea Drilling Project (DSDP) have led to suggestions that Hess and Shatsky Rises (on the Pacific Plate) had Farallon Plate counterparts, because the crust underlying Hess and Shatsky Rises is the same age as the basement of the respective plateaus[6].

Henderson *et al.*[2] suggested that Hess and Shatsky Rises were formed by hotspot activity coincident with the Farallon–Pacific spreading ridge. By analogy with present ridge-coincident hotspots such as the Iceland hotspot which formed paired plateaus,

it is possible that 'mirror images' of Hess and Shatsky Rises formed on the Farallon Plate. The Calera Limestone might then represent obducted slices of carbonate caps deposited on the plateaus.

Well-exposed outcrops of Calera Limestone at Permanente and Pacifica Quarries (Fig. 1) allow models of the origin of the Calera Limestone to be tested. At Permanente Quarry several large limestone sections are repeated by a complex series of faults. At Pacifica Quarry, a continuous 75-m section is exposed in a single block. A black shale horizon is present midway through the section, below which bituminous limestone is interbedded with thin tuffaceous horizons.

The light-grey facies of the Calera Limestone at these quarries dated by planktonic foraminifera as "at least Albian to Turonian"[7], is now known to extend to the Aptian. Foraminifera from the same sections suggest bathyal depths (200–1,500 m), similar to Hess and Shatsky Rises. Genera present include *Osangularia, Gyroidinoides, Gavelinella, Dorothia* and *Gaudryina*. Sponge spicules, agglutinated foraminifera, and fish debris which would characterize abyssal depths are absent[8]. At both quarries, evidence of shallow water debris is found in the older bituminous limestones. Nearby outcrops of Calera Limestone at Baldy Ryan Canyon near New Almaden also contain oolitic and bioclastic limestone of Albian age, indicating shallow water deposition[5].

A comparison of stratigraphic columns from Shatsky and Hess Rises, the mid-Pacific Mountains (DSDP Legs 32 and 62 respectively)[9,10] and the Calera Limestone reveals a similar stratigraphical progression from shallow to mid-bathyal depths. The oldest part of the Calera Limestone, dated by foraminifera from Pacifica and Permanente Quarries, is of Aptian age (115 Myr). By extrapolating sedimentation rates measured above the black shale marker horizon in Pacifica Quarry, we infer that the anoxic sediments below the horizon denote the Barremian–Aptian anoxic zone. As these outcrops probably predate the oldest recovered sediments from Hess Rise (early Albian to late Aptian), it is likely that Pacifica and Permanente Quarry are coeval with Shatsky Rise. The stratigraphy of Site 463 from the mid-Pacific Mountains is most similar to that of the Calera Limestone quarries. A distinctive sequence of Aptian carbonaceous limestone interbedded with tuffs is found at Site 463 and in the Calera Limestone, but is absent in DSDP sites from Hess and Shatsky Rises.

Samples were taken at Permanente Quarry by Courtillot *et al.*[11] for palaeomagnetic investigation. In that study, a positive 'mega-conglomerate' suggested that the magnetizations predate block tilting (the palaeomagnetic inclinations are in significantly better agreement after correction to the palaeohorizontal). New palaeomagnetic results from Permanente Quarry which confirm this interpretation are reported below. The age of the sections sampled falls within the Cretaceous normal polarity superchron. Therefore, with facing directions provided by foraminiferal dating, a unique determination of palaeolatitude can be established, assuming that the magnetizations were acquired shortly after deposition.

Thermal and alternating field demagnetization experiments reveal stable magnetizations with blocking temperatures of 500–580 °C, and median destructive fields of 30–40 mT. Magnetizations from 30 palaeontologically-dated samples suggest 7° of poleward translation over the depositional interval of 105–90 Myr (Fig. 2). Palaeolatitudes range from ~18 °N at 105 Myr to 25° N at 90 Myr. The palaeolatitude change implies plate speeds of at least of 5 cm yr^{-1}, in accord with estimates of Farallon Plate motion.

Using these new palaeomagnetic data, northern Pacific Basin plate motions[12–13], and geological accretion ages, a model terrane trajectory[14,15] can be computed for the Calera Limestone (Fig. 2). Our preferred model involves the following sequence:
(1) Deposition of the Calera Limestone on the Farallon Plate from 105 to 90 Myr between 18° and 25° N.
(2) Accretion to North America at 63 Myr.
(3) Northward translation relative to North America, driven by oblique subductions of the Farallon Plate from 63 to 10 Myr.
(4) Transfer to the Pacific Plate from 10 Myr to the present, after development of the San Andreas transform system.

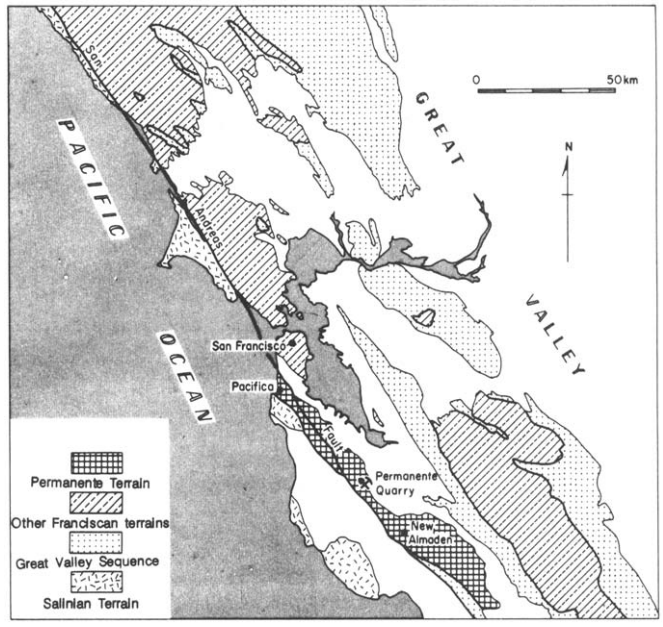

Fig. 1 Location map showing sample localities and regional relations between the Permanente Terrane, other Franciscan terranes, the Great Valley sequence, and the Salinian terrane.

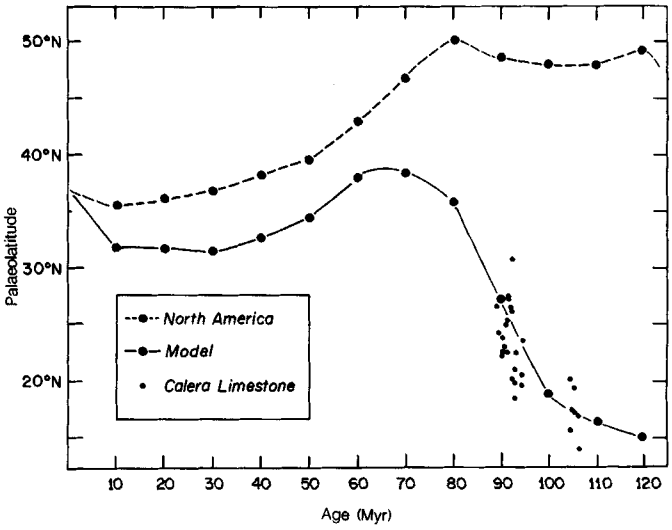

Fig. 2 A terrane model for the Calera Limestone palaeomagnetic data using the plate motion models of Engebretson *et al.*[12–13] and methods of Debiche *et al.*[14–15] The northern option for the initiation of Kula/Farallon spreading has been chosen. Palaeolatitude versus age is shown for 30 palaeontologically dated palaeomagnetic cores (small circles) of Calera Limestone from Permanente Quarry. Scatter in the data probably represents *in situ* slumping. The computed terrane model and the present location of the Calera Limestone on North America are also shown. From 106 to 63 Myr, the Calera Limestone rides on the Farallon Plate converging with North America. At 63 Myr, accretion to North America takes place. From 63 to 10 Myr, the Limestone is driven tangentially along a small circle representing the palaeo-Californian margin with 50% of the coast-parallel Farallon Plate velocity. Pacific Plate motion from 10 Myr to present takes up the final amount of northwards displacement.

The palaeopositions of Hess and Shatsky Rises during the known interval of Calera Limestone deposition can be found by reconstructing the Pacific Plate (Fig. 3). If the location of the Farallon–Pacific ridge is accurate, and if spreading is symmetrical, the symmetry between the Calera Limestone and

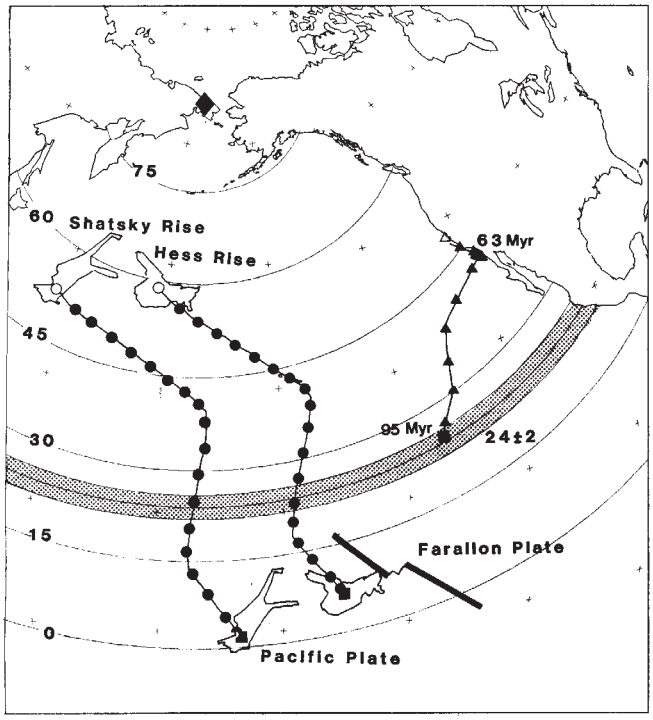

Fig. 3 Oceanic plate reconstruction in fixed North America coordinates is shown for 92 Myr. The small circles represent latitude about a 92 Myr North American pole (solid diamond) interpolated from ref. 18. Tick marks represent the present latitude and longitude coordinates, and the present coastline of Eurasia is shown for reference. Open symbols represent present-day locations while the filled squares represent positions at 92 Myr. Hess and Shatsky Rise are reconstructed back to 92 Myr on the Pacific Plate. The black circles represent 5-Myr increments. The computed terrane trajectory is shown by solid triangles. The stippled region represents the palaeomagnetic constraints for 92 Myr based on a 6-Myr averaging window. This model predicts the crust on which the Calera Limestone was deposited formed during chron M21 (153–154 Myr)[19]. Assuming an accurate location of the Farallon–Pacific ridge and symmetrical spreading, this reconstruction suggests that the Calera Limestone originated on a Farallon Plate analogue of Shatsky Rise.

Shatsky Rise astride the Pacific–Farallon ridge suggests that the plateau carrying the Calera Limestone formed as a mirror image of Shatsky Rise.

This overview, together with palaeontological and palaeomagnetic information, suggests a model for the evolution of the Permanente Terrane as a whole. In Kimmeridgian to Albian times (154–105 Myr), topographic highs (a seamount province) were formed on the Farallon Plate, possibly by a hotspot coincident with the Farallon–Pacific ridge. Although the distinction between plateaus, aseismic ridges, and seamounts is partly artificial[16], it is possible that such Farallon Plate topographic expressions attained the dimensions of present oceanic plateaus (800–1,200 km^2). General subsidence marked the Albian to Turonian interval (105–90 Myr), with the deposition of pelagic limestones and sporadic off-ridge volcanism.

Accretion in the Franciscan Complex took place in the late Cretaceous to Eocene, marked by the influx of continentally derived greywacke. The partial subduction of buoyant oceanic plateaus and seamounts could have contributed to the shallowing of the angle of subduction which was manifested by Laramide orogenic deformation[17]. As the plateaus encountered the trench, the limestone, basalt, and greywacke were obducted and imbricated by thrust faulting. Further northward translation by proto-San Andreas motion, driven by oblique subduction of the Farallon Plate, dissected the obducted limestones and juxtaposed other exotic blocks of limestone, greenstone and chert originally located on more distant parts of the Farallon Plate.

We thank Steve Kupferman and Kaiser Permanente Cement Co. for providing access to Permanente Quarry and helpful information. This research was supported by NSF grant EAR-8408035 and Petroleum Research Fund grant 13646-AC2 to McWilliams.

Received 18 March; accepted 25 July 1985.

1. Jenkyns, H. C. *J. geol. Soc., Lond.* **137**, 171–188 (1980).
2. Henderson, L. J., Gordon, R. G. & Engebretson, D. C. *Tectonics* **3**, 121–132 (1984).
3. Livaccari, R. F., Burke, K. G. & Sengor, A. M. C. *Nature* **289**, 276–278 (1981).
4. Blake, M. C. Jr, Howell, D. G. & Jayko, A. S. *Franciscan geology of Northen California* (ed. Blake, M. C. Jr) 5–22 (Pacific Section, Society of Economic Geologists and Paleontologists, Los Angeles, 1984).
5. Bailey, E. H., Irwin, W. P. & Jones, D. L. *Calif. Div. Mines Bull.* **183**, 68–77 (1964).
6. Hilde, T. W. C., Isezaki, N. & Wageman, J. M. *Geophys. Mongr. Ser.* **19**, 205–226 (1976).
7. Sliter, W. V. *Pacific Sect. SEPM* **43**, 149–162 (1984).
8. Premoli-Silva, I. & Sliter, W. V. *Init. Rep. DSDP Leg* **61**, 423–437 (1981).
9. Larson, R. L. *et al. Init. Rep. DSDP Leg* **32**, 75–191 (1975).
10. Theide, J., *et al. Init. Rep. DSDP* Leg **62**, 157–326 (1981).
11. Courtillot, V. *et al. Geology* **13**, 107–110 (1985).
12. Engebretson, D. C., Cox, A. & Gordon, R. G. *J. geophys. Res.* **89**, 291–10, 310 (1984).
13. Engebretson, D. C., Gordon, R. G. & Cox, A. *Geol. Surv. Am. Spec. Pap.* (in the press).
14. Engebretson, D. C., Debiche, M. & Cox, A. *Stanford Univ. Publ. Geol. Sci.* **18**, 83–85 (1984).
15. Debiche, M. G., Cox, A. & Engebretson, D. C. *Geological Soc. Am.* Spec. Pap. **206**(2), (in the press).
16. Jenkyns, H. C. in *Sediments, Environments and Facies* (ed. Reading, H. C.) (Elsevier, New York, 1978).
17. Dickinson, W. R. & Snyder, W. S. *Bull. geol. Soc. Am.* **151**, 337–366 (1978).
18. Irving, E. & Irving, G. A. *Geophys. Surv.* **5**, 141–188 (1982).
19. Harland, W. B. *et al. Geological Time Scale* (Cambridge University Press, 1982).

Contaminated sediments of lakes and oceans act as sources of chlorinated hydrocarbons for release to water and atmosphere

Per Larsson

Institute of Limnology, University of Lund, Box 65, S-221 00 Lund, Sweden

Atmospheric transport is a major route for entry of chlorinated, aromatic hydrocarbons into aquatic ecosystems. Once in the water, the compounds are readily taken up by the biota and distributed in the food webs. Major fractions of the compounds are deposited in the sediment[1], and it had been thought that most persistent contaminants are inactivated in this way as a consequence of their lipophilic properties. However, results from recent laboratory studies[2,3] raise the possibility that aquatic sediments may not be the final sink for the substances but may rather act as a source through redistribution of the compounds to water and the atmosphere. Polychlorinated biphenyls (PCBs) may be regarded as 'tracers' for these contaminants in the ecosystem, and I studied the transport of PCBs from sediment to water and air in two artificial ponds in the field. The transport from the sediment followed a seasonal cycle; higher concentrations of PCBs in water and air were recorded in the summer and lower in the winter. PCB concentrations in the air over the ponds were positively correlated with PCB levels in the water. My results show that contaminated sediments may act as a source of chlorinated hydrocarbons released into the environment.

In laboratory model systems PCBs are transferred across the sediment/water interface by processes including bioturbation (the activity of benthic macroinvertebrates in the sediment), desorption and gas convection[2,3]. PCBs also volatilize from water to the air[4] and a potential cycle of PCBs across the boundaries sediment/water and water/air is thus established. A similar cycle has been proposed for chlorobenzenes in the Niagara River and Lake Ontario[5].

Transport of PCBs from the sediment to the water and air was studied in large outdoor model ecosystems located in southern Sweden. The systems consisted of two pools (diameter 7.3 m, volume 50 m^3), to each of which I added 5–6 tons of lake sediment. The PCB compounds (12 g Clophen A 50, dissolved in 1 l of ethanol) were thoroughly mixed by blending 50 ml of the PCB solution into sections of the sediment. The entire sediment was then stirred with a rake and left for 1 week to